Functional Materials Letters
(2023) 2350013 (5 pages)
© World Scientific Publishing Company
DOI: 10.1142/S1793604723500133

World Scientific
www.worldscientific.com

Actuation behavior of PNIPAM-based bilayer hydrogel regulated by polyvinyl alcohol polymer film

Jiaxin Li*, Ruofei Wang*, Diqing Ruan*, Huaping Wu†, Lin Cheng* and Aiping Liu*,‡

*Key Laboratory of Optical Field Manipulation of Zhejiang Province
Zhejiang Sci-Tech University, Hangzhou 310018, P. R. China
†Key Laboratory of Special Purpose Equipment and Advanced Processing Technology
Ministry of Education and Zhejiang Province, College of Mechanical Engineering
Zhejiang University of Technology, Hangzhou 310023, P. R. China
‡liuaiping1979@gmail.com

Received 7 February 2023; Revised 5 April 2023; Accepted 14 April 2023; Published 17 May 2023

Responsive hydrogels based on Poly(N-isopropylacrylamide) (PNIPAM) are known to exhibit distinctive thermosensitive properties. However, isotropic PNIPAM hydrogels with weak mechanical properties and low deformation rates tend to exhibit only regular volume expansion/contraction, which limits them to promising applications such as intelligent actuators. In order to prepare programmable hydrogel actuators with satisfactory mechanical properties and fast deformation capability, a polyvinyl alcohol/PNIPAM (PVA/PNIPAM) bilayer hydrogel with anisotropic structure is proposed by combining preprepared PVA polymer film with outstanding mechanical properties as the passive layer and thermosensitive PNIPAM hydrogel as the active layer, forming a semi-interpenetrating network structure at the interface via the hydrogen-bond interaction between PNIPAM and PVA. The microstructures, mechanical properties and actuation behaviors of bilayer hydrogel were studied by scanning electron microscope, Fourier transform infrared spectrograph, mechanical testing machine and actuation test device. Results show that the introduction of PVA can improve the tensile stress of the bilayer hydrogel from 23.6 kPa to 62.6 kPa, and favor the hydrogel actuator excellent actuation preformation with a maximum bending amplitude of 500° and a maximum bending velocity of 13°/s within first 40 s. The bilayer hydrogel is further designed to work as a fluidic system valve that can recognize various temperature solutions and control solution flow rate. This design provides a simple and practical strategy to construct responsive hydrogels with anisotropic structure for further development in the field of intelligent actuators and flexible microfluidic systems.

Keywords: PNIPAM hydrogel; PVA polymer film; bilayer structure; actuation performance; smart valve.

Funct. Mater. Lett. Downloaded from www.worldscientific.com
by ZHEJIANG UNIVERSITY on 05/24/23. Re-use and distribution is strictly not permitted, except for Open Access articles.

Smart hydrogels with modulus similar to that of living organisms are considered as one of ideal materials for soft robots,[1,2] which also have unlimited possibilities used in microfluidic valves,[3] drug delivery systems,[4] multifunctional sensors,[5,6] and smart actuators.[7,8] Under external stimuli, including temperature,[9,10] magnetic field,[11,12] electric field,[13,14] pH,[15,16] light,[17,18] or ions,[19,20] responsive hydrogels are capable of producing controlled volume and shape changes. However, pure hydrogels with isotropic structure tend to have poor mechanical properties and exhibit only regular volume expansion/contraction. To achieve bending, twisting, and crawling deformations, the construction of anisotropic hydrogels with satisfactory mechanical properties and fast deformation capability is first and foremost.

At present, various hydrogels with anisotropic structures including oriented structure,[7] gradient structure,[21] and bilayer structure,[22] have been proposed. For example, Zheng *et al.* constructed oriented structured hydrogel by complex 3D printing techniques, realizing the hydrogel programmable deformation and mechanical properties improvement. [7] Dong *et al*. constructed a heterogeneous porous hydrogel with specific shape variations by diffusion of different liquids (e.g. pentanol, water, and so on) into the monomeric precursor solution of the Poly(N-isopropylacrylamide) (PNIPAM) hydrogel.[23] This inhomogeneous porous structure leads to the deterioration of its mechanical properties to some degree. Xu *et al*. prepared biologically inspired thermosensitive hydrogel actuators with a bilayer structure by applying textured dust-free paper as the passive layer to achieve fast, reversible, and controlled programmed deformations.[24] However, this bilayer structure has still the stratification possibility after repeated cycles of bending deformation. An enhanced interface interaction should therefore be considered. Based on this, we provide a simple and general method to construct a bilayer hydrogel with anisotropic structure by using polyvinyl alcohol (PVA) polymer film with outstanding mechanical

‡Corresponding author.

Funct. Mater. Lett. Downloaded from www.worldscientific.com
by ZHEJIANG UNIVERSITY on 05/24/23. Re-use and distribution is strictly not permitted, except for Open Access articles.

properties as the passive layer and PNIPAM nanocomposite hydrogel as the active layer. Compared to dust-free paper/PNIPAM bilayer structure, strong intermolecular hydrogen bonds can be formed between the rich hydroxyl groups of PVA and amide groups of PNIPAM, resulting in a semi-interpenetrating network structure at the interface between PNIPAM and PVA. This PVA introduction also excellently improves the tensile stress and actuation performance of the PVA/PNIPAM composite hydrogel. The application of bilayer hydrogel as intelligent valves in the intelligent fluidic systems is investigated.

The synthesis scheme for PVA/PNIPAM composite hydrogel is shown in Fig. 1. Typically, 0.226 g of 1-hydroxycyclohexyl phenyl ketone (Irg.184) was added to 10 mL of methanol solution and stirred for 0.5 h to obtain the photoinitiator. Then 1.14 g of nano-clay (Laponite XLG), 5.65 g of N-isopropylacrylamide (NIPAM, 99%), and 500 μL of photoinitiator were stirred in deionized water until obtaining uniform hydrogel precursor solution. A mold consisting of two slides (60 mm × 25 mm) and a silica gel spacer with a hollow of 40 mm × 10 mm was prepared, and the thickness of the silica gel spacer was controlled as 1, 1.5, 2, and 2.5 mm, respectively. The prepared hydrogel precursor solution was injected into the above mold and the molds were placed in an ice-water bath illuminated by a UV lamp (λ = 365 nm, 250 W) for 5 min. 2 g of PVA was added into 98 mL of deionized water and heated in a 60°C water bath for 2 h until all PVA was dissolved, and then 10 mL of PVA solution to the Petri dish was taken to obtain a PVA film (40 mm × 10 mm × 100 μm) after 60°C evaporation. After demolding the cross-linked PNIPAM hydrogels, the samples were laminated with the prepared PVA film and chemically cross-linked in 1% glutaraldehyde solution at room temperature for 8 h. During this process, the PVA film was partly hydrolyzed and infiltrated into the PNIPAM network, forming the PVA/PNIPAM bilayer hydrogels with a semi-interpenetrating network structure at the interface. By changing the thickness of the silica gel spacer, the PVA/PNIPAM$_x$ (x = 1, 1.5, 2, and 2.5) hydrogels with different thicknesses were prepared. All the chemical agents used in the experiment process were purchased from Shanghai Aladdin reagent Co., LTD (China) and were checked for analytical purity without further processing.

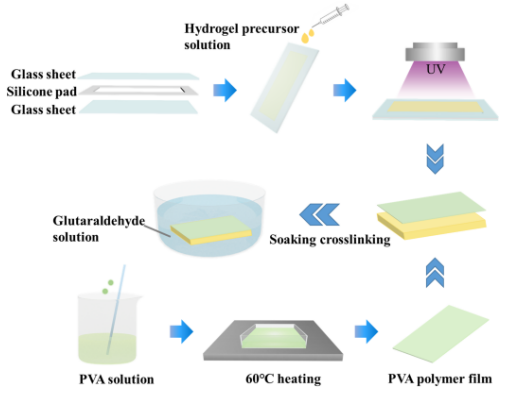

Fig. 1. Synthesis of the PVA/PNIPAM bilayer hydrogel.

A scanning electron microscopy (SEM, S-4800, Hitachi, Tokyo, Japan) was used to observe the microstructures of PVA/PNIPAM bilayer hydrogels after the samples were frozen in the liquid nitrogen and freeze-dried in a freeze-dryer (Shanghai Leewen Scientific Instrument Co., Ltd.) at −80°C. The functional groups of the bilayer hydrogels were determined by a Fourier transform infrared spectroscopy (FTIR, Nicolet iS50 Series) in the range from 500 cm^{-1} to 4000 cm^{-1}. Stretching experiments were performed on a mechanical testing machine (Instron 5943, USA) with a tensile specimen (40 mm × 10 mm × 1 mm) at a tensile speed of 50 mm/min. The lower critical transition temperature (LCST) of bilayer hydrogel was analyzed on a differential scanning calorimeter (DSC, TA DSC Q200, USA) by heating the sample from 20°C to 50°C at a scanning rate of 5°C min^{-1} under a nitrogen atmosphere. The volume shrinkage of hydrogels was calculated by area and bulk at different time intervals in optical pictures. The PVA/PNIPAM hydrogel sheets were cut to 1 cm × 1 cm and immersed into the 50°C water. The thermos-responsive volume change of PVA/PNIPAM hydrogels was recorded by a digital camera at different time intervals.

To investigate the driving deformation behavior of the PVA/PNIPAM bilayer hydrogel, one end of the sample was clamped while the other was free-floating in the air. The bilayer hydrogel was then placed in deionized water at 50°C to bend, then in deionized water at 20°C to recover after bending to the maximum displacement. The images at different time points were intercepted, and the bending amplitudes of the bilayer hydrogels in the screenshots were measured by Image J software. The circular angle α in the bending state was defined as the actual bending amplitude of the bilayer hydrogel. Image J software was used to measure the angle θ between the tangents of the two ends of bilayer hydrogel in the bending state, and the actual bending amplitude could be calculated according to the formula $\alpha = 2\theta$.

Figure 2 shows the SEM images of the PVA/PNIPAM bilayer hydrogel. The SEM cross-sectional images confirm the apparent bilayer structure of PVA/PNIPAM hydrogels (Figs. 2(a) and 2(b)). The top layer is a homogenous PVA film with a thickness of about 100 μm, and the bottom layer is the PNIPAM hydrogel with a uniform porosity structure. These two layers are firmly bonded together (Fig. 2(b)). The top and bottom surfaces of bilayer hydrogel also exhibit the properties of a homogeneous membrane (Fig. 2(c)) and porous structure (Fig. 2(d)).

The functional groups of the bilayer hydrogels are determined by the FTIR. The absorption peaks at about 1460, 1543, and 1645 cm^{-1} are corresponding to the absorption peaks of

Funct. Mater. Lett. Downloaded from www.worldscientific.com
by ZHEJIANG UNIVERSITY on 05/24/23. Re-use and distribution is strictly not permitted, except for Open Access articles.

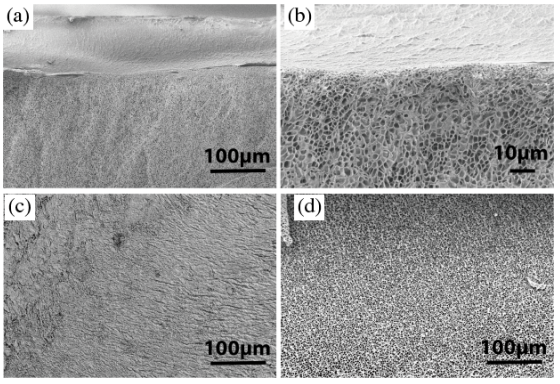

Fig. 2. SEM images of PVA/PNIPAM hydrogels: (a) overall cross-section, (b) magnification of the bilayer hydrogel interface, (c) top surface, and (d) bottom surface of bilayer hydrogel.

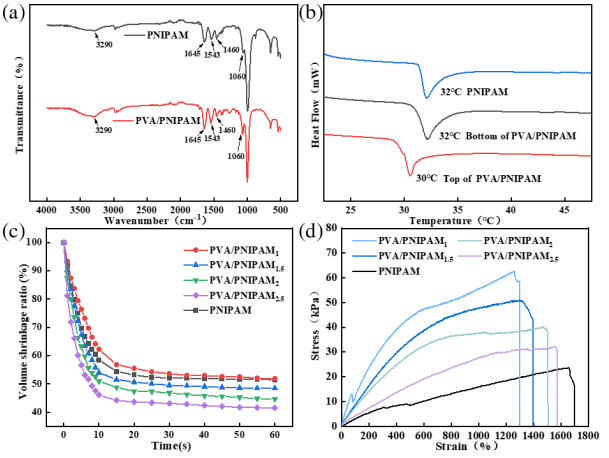

Fig. 3. (a) FTIR spectra of PNIPAM and PVA/PNIPAM hydrogels. (b) DSC curves of PNIPAM hydrogel and top and bottom parts of PVA/PNIPAM hydrogels. (c) Volume shrinkage ratio of PNIPAM and PVA/PNIPAM$_x$ (x = 1, 1.5, 2, and 2.5) hydrogels in 50°C hot water. (d) Tensile stress-strain curves of PNIPAM and PVA/PNIPAM$_x$ hydrogels.

–CH(CH$_3$)$_2$ stretching vibration, –NH$_2$ bending vibration, and C=O stretching vibration in PNIPAM.[25] Comparing to PNIPAM hydrogels, the O–H contraction vibrations of PVA/PNIPAM hydrogels increases in the range of 3200–3500 cm^{-1}, while the corresponding –CH(CH$_3$)$_2$ groups at 1460 cm^{-1} decreases in intensity. The reason for this change could be the introduction of hydroxyl-rich PVA material, where the hydroxyl group of PVA forms a stronger hydrogen bonding interaction with the C=O of PNIPAM, inhibiting the binding of –NH$_2$ and C=O of PNIPAM.[26] While after chemical cross-linking with glutaraldehyde, the two aldehyde groups of the glutaraldehyde molecule can contact more hydroxyl groups, leading to the condensation of aldehyde groups, which is manifested by an increase in the aldehyde groups (C–O–C) at 1060 cm^{-1}.[27] This hydrogen bonding interaction between PVA layer and PNIPAM layer leads to a better compatibility of PNIPAM with PVA, forming a semi-interpenetrating network structure at the interface (Fig. S1).

In order to study the effect of PVA to LCST of bilayer hydrogel, the DSC tests were performed on the top and bottom layers of bilayer hydrogels. The bottom of the bilayer hydrogel still maintains the same LCST of pure PNIPAM hydrogel (32°C), while the LCST of the top of the bilayer hydrogel with PVA introduction reduces to 30°C (Fig. 3(b)). For PNIPAM hydrogel, the polymer chains are the combination of hydrophobic and hydrophilic chain segments. The addition of glutaraldehyde decreases the distance between PVA chains and increases their interaction.[25] The hydrogen bonding between hydroxyl groups of PVA and C=O groups of PNIPAM is enhanced, while the stability of –NH$_2$ and C=O of the hydrophilic PNIPAM is reduced. When hydrogen bonds are broken, hydrophobic interactions between PNIPAM chains dominate.[26] This may be the reason for the decrease of LCST after the introduction of PVA at the top of bilayer hydrogel.

In addition, the bilayer structure also affects the water loss rate of the hydrogel, which further affects the driving performance of the hydrogel actuator. Since PVA is not a thermosensitive material, the variation in the water loss rate of the bilayer hydrogel is caused by the thermally responsive behavior of PNIPAM hydrogel. As demonstrated in Fig. 3(c), PVA addition prevents the swelling of the molecular chains of PNIPAM hydrogel to some extent, reducing the water loss rate of the PVA/PNIPAM$_1$ hydrogel. As the thickness of PNIPAM hydrogel increases, the swelling difference between the PVA layer and PNIPAM layer increases, the limited impact of PVA reduces, and the water loss rate of PVA/PNIPAM$_x$ hydrogel (x = 1.5, 2, 2.5) increases. The effect of PVA film on the mechanical properties of bilayer hydrogels was further investigated. As shown in Fig. S2, the PVA film has a tensile stress up to about 10 MPa, while the strain is only about 320%. The PNIPAM hydrogel with nanoclay as a cross-linking agent usually has a good tensile strain with a strain energy of 1731% (Fig. 3(d)). However, it has poor mechanical properties with a tensile stress of only 23.6 kPa due to the high water content in the hydrogel. As shown in Figs. S3, S4, and 3(d), the tensile stress of the bilayer hydrogel greatly improves since the combination of PVA film, resulting in a higher cross-link density at the top, and a decrease in elongation at break and an increase in tensile stress (62.6 kPa). With the thickness increase of PNIPAM hydrogel, the percentage of PVA becomes smaller and its influence on the bilayer hydrogel becomes smaller, leading to a decrease of tensile stress of bilayer hydrogels.

When the PVA/PNIPAM bilayer hydrogel with an anisotropic structure is placed in deionized water at 50°C, the PVA layer hinders the volume contraction of the PNIPAM hydrogel layer, causing the bilayer hydrogel to bend toward the PNIPAM side. Figures 4(a)–4(d) show that the bending velocity and the maximum bending amplitude decrease as

Funct. Mater. Lett. Downloaded from www.worldscientific.com
by ZHEJIANG UNIVERSITY on 05/24/23. Re-use and distribution is strictly not permitted, except for Open Access articles.

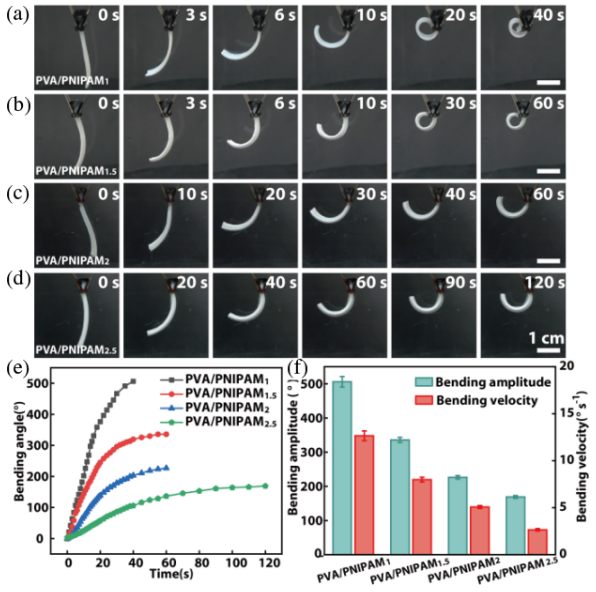

Fig. 4. (a)–(d) Optical photographs of bending process of the PVA/PNIPAM$_x$ (x = 1, 1.5, 2, and 2.5) hydrogels in hot water at 50°C. (e) The relationship between bending amplitude and time of different PVA/PNIPAM$_x$ hydrogels in hot water. (f) Overall bending amplitude and the initial bending velocity during the first 40 s for different PVA/PNIPAM$_x$ hydrogels in hot water.

the thickness of PNIPAM hydrogel layer increases. This is because under the same 50°C deionized water condition, the self-weight of the bilayer hydrogel increases with the increase of PNIPAM thickness, the resistance to be overcome by the actuator increases, and the actuation capacity becomes worse. When the thickness of the PNIPAM hydrogel is 1 mm, the bilayer hydrogel can obtain the fastest actuation velocity of 13°/s within the first 40 s and the maximum bending amplitude of 500° (Figs. 4(e) and 4(f)). We performed up to 20 repeated experiments of actuation/reversion tests in the water environment and stretching/releasing tests by the mechanical machine, respectively, for the PVA/PNIPAM bilayer hydrogel. SEM images show that the bilayer interface is tightly bonded without obvious delamination after multiple experiments (Fig. S5). This indicates a strong interfacial interaction between the bilayers. By comparing the mechanical and

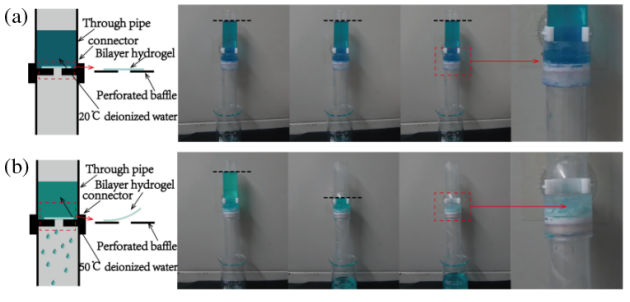

Fig. 5. Schematic diagram and optical photos of an intelligent valve controlling liquid inflow: (a) schematic diagram and optical photos of intelligent valve action at 20°C deionized water, (b) schematic diagram and optical photos of intelligent valve action at 50°C deionized water.

actuation performances of different hydrogels as actuators, the results show the great advantages of our hydrogel as an actuator (Table S1).[7–10,16–18,21,22,28]

Based on the above experiment result, an intelligent fluidic system is designed and fabricated using PVA/PNIPAM$_1$ bilayer hydrogel as a valve switch (Fig. 5). The system consists of a baffle with a small hole (the diameter of 5 mm) in the center, through two pipes with a diameter of 3 cm, a connector connecting the two pipes, and a PVA/PNIPAM$_1$ hydrogel valve switch (1 mm × 2 cm × 2 cm). The intelligent valve system is controlled by the bilayer hydrogel (the PNIPAM layer side faces upward and is placed directly above the small hole baffle), which is fixed at one end and freely movable at the other. When 20°C deionized water is injected into the valve pipe, the hydrogel valve does not get the "release" command, at the same time in the role of liquid pressure, the hydrogel valve switch tightly closes the small hole without deionized water passing through the small hole. When 50°C deionized water is passed into the valve pipe, the hydrogel valve receives the temperature "release" command and the active end is bent upward to expose the small hole, and 50°C deionized water is circulated through the small hole. The intelligent fluidic system with a hydrogel valve uses the temperature as the command and the bending and deformation of the hydrogel to realize the system control. Changing the thickness of bilayer hydrogel can further adjust the opening and closing speed of the smart valve, and therefore control the flow velocity of high-temperature liquid. This indicates the good application prospects of PVA/PNIPAM bilayer hydrogel in the field of intelligent fluidic systems.

In summary, the PVA/PNIPAM bilayer hydrogels with anisotropic structure were prepared by combining PVA polymer film and PNIPAM hydrogel. Due to the incorporation of PVA polymer film, the tensile stress was increased by 3 times compared with PNIPAM hydrogel. The maximum bending velocity of the bilayer hydrogel was about 13°/s and the maximum bending amplitude was about 500°, showing remarkable properties such as fast driving and wide bending amplitude. The design of an intelligent valve system using bilayer hydrogel confirmed its application possibilities in intelligent fluid systems and provided design inspiration for the double-layer hydrogel actuator used in areas such as soft robotics, artificial muscles, and intelligent human-machine technology. Further experimental exploration will be carried out to obtain a universal approach to construct anisotropic hydrogels with different responsiveness by adjusting the type of hydrogel or polymer membrane.

Acknowledgment

This work was supported by the National Natural Science Foundation of China (Nos. 12272351 and 11972323), the

Youth Top-notch Talent Project of Zhejiang Ten Thousand Plan of China (No. ZJWR0308010), and the Zhejiang Provincial Natural Science Foundation of China (Nos. LR19E020004 and LR20A020002).

References

1. H. Cui *et al*., *Adv. Intell. Syst.* **2**, 2000138 (2020).
2. M. Ilami *et al.*, *Adv. Mater.* **33**, 2003139 (2021).
3. N. Tao *et al*., *Chem. Sci.* **10**, 10765 (2019).
4. Z. Han *et al.*, *ACS Appl. Mater. Interfaces* **12**, 12010 (2020).
5. H. Y. Peng *et al*., *J. Mater. Chem. C* **6**, 11356 (2018).
6. Y. Qiu *et al.*, *Nano Energy* **78**, 105337 (2020).
7. S. Y. Zheng *et al.*, *Adv. Funct. Mater.* **28**, 1803366 (2018).
8. Q. Zhao *et al.*, *J. Mater. Chem. B* **6**, 1260 (2018).
9. X. He *et al*., *J. Mater. Chem. C* **7**, 4970 (2019).
10. L. Hua *et al.*, *ACS Appl. Mater. Interfaces* **11**, 43641 (2019).
11. D. Zhang *et al.*, *Adv. Intell. Syst.* **3**, 2000208 (2021).
12. Z. Q. Zhang *et al.*, *Funct. Mater. Lett.* **15**, 2250022 (2022).
13. D. Han *et al.*, *ACS Appl. Mater. Interfaces* **10**, 17512 (2018).
14. S. Wei *et al.*, *ACS Nano* **15**, 10415 (2021).
15. T. Cui *et al*., *Adv. Sci.* **9**, 2201254 (2022).
16. C. Ma *et al.*, *Adv. Funct. Mater.* **28**, 1704568 (2018).
17. R. Yu *et al*., *Adv. Mater. Interfaces* **9**, 2200401 (2022).
18. C. Zheng *et al.*, *Sens. Actuators B, Chem.* **304**, 127345 (2020).
19. S. Y Zheng *et al.*, *Adv. Funct. Mater.* **28**, 1803366 (2018).
20. G. Xu *et al*., *Adv. Funct.* **32**, 2109597 (2022).
21. Y. Gao *et al.*, *Macromol. Chem. Phys.* **223**, 2100117 (2022).
22. K. Liu *et al*., *Adv. Mater.* **32**, 2001693 (2020).
23. P. L. Dong *et al.*, *Adv. Intell. Syst.* **3**, 2640 (2021).
24. W. Z. Xu *et al.*, *Sens. Actuators B, Chem.* **359**, 131547 (2022).
25. D. Morales *et al.*, *Soft Matter* **10**, 1337 (2014).
26. J. Zhang *et al*., *Polymer* **253**, 124998 (2022).
27. K. Figueiredo *et al.*, *J. Appl. Polym. Sci.* **111**, 3074 (2009).
28. Y. Zheng *et al.*, *Chem. Eng. J.* **454**, 140054 (2023).

Funct. Mater. Lett. Downloaded from www.worldscientific.com
by ZHEJIANG UNIVERSITY on 05/24/23. Re-use and distribution is strictly not permitted, except for Open Access articles.